

3a1-3

The optical design of HIMAC secondary beam course

Masahito Hosaka, Koji Noda, Takeshi Murakami, Mitsutaka Kanazawa,
Atsushi Kitagawa, Yukio Sato, Eiichi Takada, Masami Torikoshi
and Satoru Yamada

National Institute of Radiological Sciences
4-9-1 Anagawa, Inage-ward, Chiba-city, Chiba-prefecture, 263, Japan

ABSTRACT

A new beam course is under construction in HIMAC, NIRS, in order to utilize radioactive secondary beams for medical purpose. The new course comprises a doubly achromatic spectrometer, which separates projectile fragmentations. The design and the beam optics are presented.

1. INTRODUCTION

Application of radioactive beams[1] is related to vast scientific areas, and one of the fruitful candidates is a medical use. The heavy-ion accelerator complex for medical use, HIMAC, began its operation in 1994 and continues treatment of cancer patients[2]. Great advantages of charged-particle therapy, especially by heavy ions, are the excellent dose distribution and the high biological effectiveness.

Although ranges and scattering angles in various materials can be, in principle, precisely evaluated, small ambiguities are left in evaluation of the dose distribution inside human bodies because they are complicated mosaic of soft and hard tissues. In order to fully utilize the advantage of the charged particles, precise measurements and/or confirmation of dose distribution inside bodies under practical conditions are important.

Combination of radioactive secondary beams of positron emitters and annihilation γ -ray detectors like PETs will realize these measurements with no excessive dose. Beams of ^{11}C and ^{19}Ne are good candidates for this purpose and are mainly quoted in the design stage of the new course. On the other hand, other types of beams, especially heavier ones, are taken into consideration in order to expand experimental fields being carried out by the new course. Therefore beam optics of three beam courses are studied in order to maintain the versatility in the future. One of the new courses is now under construction and will be completed in three years. This paper describes design and beam optics of the new course.

2. BEAM OPTICS AND LAYOUT

Layout of the new course A layout of the new course is illustrated in Fig. 1. The new beam course is a double-achromatic fragment separator, comprising two bending magnets, 11 quadrupole magnets, and an energy degrader.

The reaction products produced in the production target, are separated from the primary beam by a 20° bending magnet (BM01). The maximum magnetic rigidity is chosen to be 8.13 Tm, which corresponds to $q/A = 1/2$ ions with an energy of 600 MeV/nucleon.

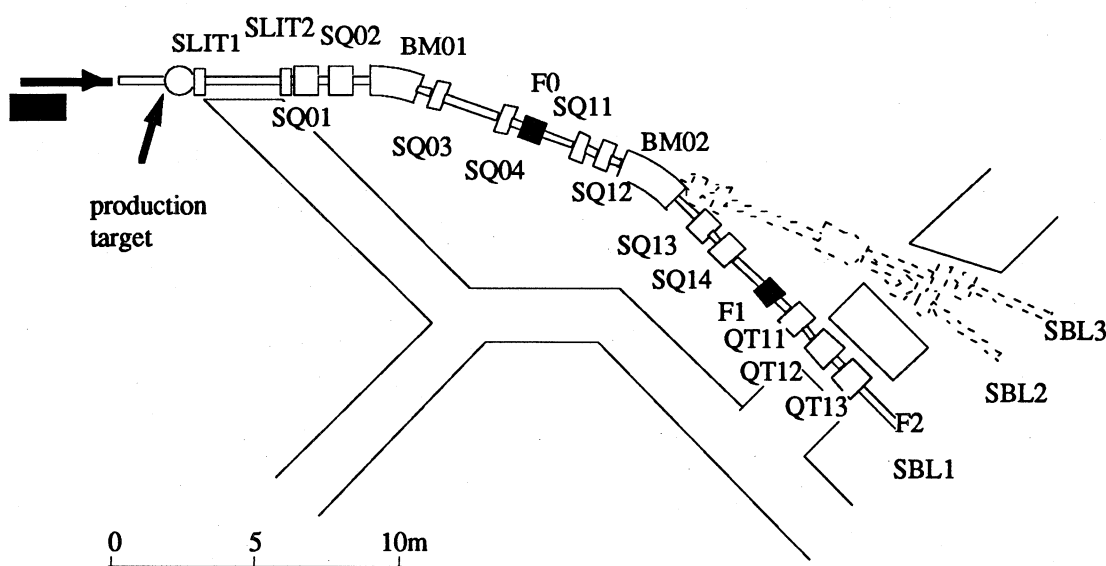


Fig. 1 Layout of HIMAC secondary beam course. The course denoted by "SBL1" is now under construction.

Dumping locations of primary beams vary dependent on their magnetic rigidity relative to that of a secondary beam. Most of primary beams are stopped by a movable beam stopper placed between an exit of the magnet, BM01, and an entrance of a quadrupole magnet, SQ04. The exact separation of the fragments is performed at a dispersive focusing position F0 where the fragments with different magnetic rigidity are focused on the different position. The dispersion D at F0 is taken to be the value of 1.87 (cm/%). With an object size $x_0 = \pm 0.3\text{cm}$, at the production target, and then at F0 the image size $x = (x,x)x_0 = \pm 0.28\text{cm}$, the momentum resolution is $R = 2x/D = 0.30\%$. An achromatic energy degrader of a wedge in shape can be inserted at F0, which allows an additional fragment separation at the later stage.

The second magnet, BM02, with a bending angle of 26.5° and a pair of quadrupole magnets realize the double achromatic condition that two chromatic terms (x,p) and (x',p) vanish hereafter. Thus, the image size of the secondary beam, which is broadened owing to its own momentum spread at the dispersive focus F0, once more shrink. When an achromatic energy degrader is placed at F0, an additional isotope separation can be performed at the second focusing point F1. This second selection based on the difference of the atomic energy loss in the degrader, is essential for the separation of fragments of heavier nuclei with whose magnetic rigidity one cannot identify.

The three last quadrupole magnets gives the third focus at F2 where irradiation of the radioactive secondary beam is performed for medical purpose or for other scientific research. The flexibility of using three quadrupole magnets allow the focusing position to vary to meet various requirements.

As shown in Fig. 1., whole system is not symmetric due to constraint that three beam courses should be made within limited space. Although the optimization process to attain double achromatic condition may need a longer time than that of the symmetric case, it essentially gives the same properties. The beam optics was calculated using the code MAGIC[3]. The design parameters and values of matrix elements are summarized in Table 1 and the first order beam envelopes are shown in Fig. 2.

Table 1
The parameters of the secondary beam course

Angular acceptance	
vertical	± 13 mrad
horizontal	± 13 mrad
Momentum acceptance	$\pm 2.5\%$
Max. magnetic rigidity	8.13 Tm
Flight path length	11.9m to F0
	22.6m to F1
	29.4m to F2

The ion optical matrix elements ^{a)}			
Matrix element	F0	F1	F2
(x,x)	-0.93	0.87	-0.35
(x,x') [cm/mrad]	-0.000	0.000	0.000
(x,p) [cm/%]	-1.87	0.000	0.000
(x',p) [mrad/%]	-0.26	0.000	0.000
(y,y)	-1.75	0.86	-2.1
(y,y') [cm/mrad]	0.029	0.010	0.000

^{a)} The matrix elements transfer initial values of x_0, x'_0 and p_0 as following.

$$\begin{pmatrix} x \\ x' \\ p \end{pmatrix} = \begin{pmatrix} (x,x) & (x,x') & (x,p) \\ (x',x) & (x',x') & (x',p) \\ (p,x) & (p,x') & (p,p) \end{pmatrix} \begin{pmatrix} x_0 \\ x'_0 \\ p_0 \end{pmatrix}$$

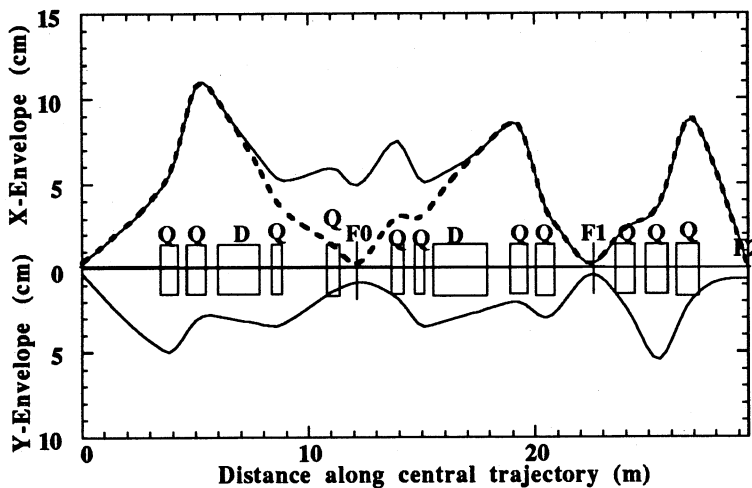


Fig. 2. The first order beam envelopes calculated for a initial parallelogram-like emittance of ± 13 mrad in angle and $\pm 3\text{mm}$ in size

Solid line : with momentum spread $\pm 2.5\%$
Dashed line : without momentum spread

Acceptance In general large values of beam emittance and momentum spread are unavoidable in secondary beams. Therefore wide acceptance is needed to collect a larger amount of all the fragment. These angular and momentum spread of the secondary beam are estimated based on the statistical model of Goldhaber[4]. Consequently the acceptance values of $\pm 13\text{mrad}$ both horizontal and vertical angle, and $\pm 2.5\%$ in momentum are chosen. With these values, the fragment separator can transport as secondary beam, 65% of ^{11}C and 90% of ^{19}Ne fragments produced in the reaction that a 5cm-thick beryllium target are bombarded with 600MeV/nucleon ^{12}C and ^{20}Ne primary beams respectively.

Second order calculation An optics of an ion optical system with a wide acceptance, might be affected by the higher order aberration greatly. Hence we evaluated the second order aberration for the secondary beam course using the code GIOS[5] and the following effects were found. First, the focal plane at F0 is slightly tilted relative to the perpendicular plane to the optical axis. Although this aberration deteriorates the momentum resolution at F0, it was confirmed that degrading of the ability is negligible for the separation of nuclei such as ^{11}C or ^{19}Ne . Second, the image size is found to increase owing to the second order aberration, especially at the focusing points. As an example, the calculated position distribution of the secondary beam of ^{11}C at the second focus F1 is shown in Fig. 3. The secondary beam is assumed to be initially distributed of Gaussian shape in position, angle and momentum space, whose widths are determined under the condition that the secondary beam is produced by a bombardment of a primary beam of 600MeV/nucleon ^{12}C with a 5cm thickness beryllium target. As shown in the figure, the second order aberration does not make much difference to the position distribution of the secondary beam, except for a rather long outer tail. This tail may have a harmful effect for the separation of the fragments with very small production cross section from those with large production cross section, but in most of case the effect is expected to be of little importance.

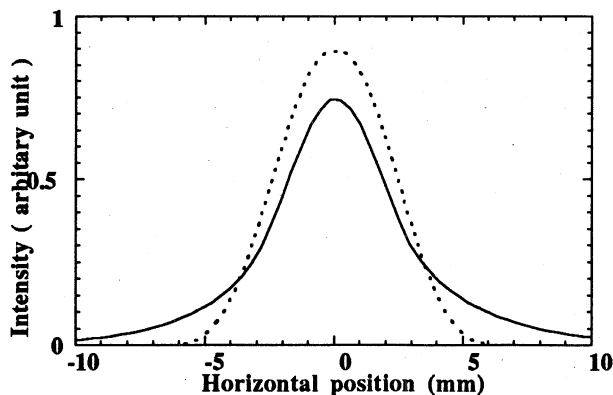


Fig. 3. Calculated ^{11}C beam position distribution at F1.
 Solid line : the second order calculation
 Dashed line : the first order calculation

ACKNOWLEDGEMENTS

The authors would like to thank Dr. K. Kawachi for his encouragement and helpful advice.

REFERENCES

- [1] T. Kubo et. al., Nucl. Instr. and Meth. B70 (1992) 309
- [2] K. Sato et. al., Nucl. Phys. A588 (1995) 229c-234c
- [3] A. S. King et. al., SLAC-183-RL-75-110 (1975)
- [4] A. S. Goldhaber, Phys. Lett. B53 (1974) 306.
- [5] H. Wollnik et al., Nucl. Instr. and Meth. A258 (1987) 408.